# Conductivity of the interface for spin-polarized electrons in the pseudogap state of underdoped $YBa_2Cu_3O_x$

P. Mikheenko
*School of Engineering, University of Birmingham, Edgbaston, Birmingham, B15 2TT, United Kingdom*

R. Chakalova and C. M. Muirhead
*School of Physics and Astronomy, University of Birmingham, Edgbaston, Birmingham, B15 2TT, United Kingdom*
(Received 22 September 2004; revised manuscript received 18 January 2005; published 27 May 2005)

We report resistance-temperature, conductance-voltage, and voltage–magnetic-field measurements in a range of small-area junctions between colossal magnetoresistive materials and the high-temperature superconductor $YBa_2Cu_3O_x$ (YBCO). We identify two forms of behavior. In one form the resistance of the junction falls with decreasing temperature and is associated with zero bias conductance peaks. In the other form the resistance rises below some characteristic temperature $T^*$. In this latter case there is no zero bias conductance peak, but there are small peaks in the voltage–magnetic-field behavior below $T^*$. We tentatively associate $T^*$ with the pseudogap temperature and argue that the observed effects result from an interaction between the spin-polarized current and the antiferromagnetic spin fluctuations of the pseudogap state.

DOI: 10.1103/PhysRevB.71.184517 PACS number(s): 74.72.Bk, 74.78.Bz, 85.75.−d, 74.45.+c

## I. INTRODUCTION

There has recently been much interest in the effect of spin-polarized injection on the superconducting state of conventional and unconventional superconductors. This has concentrated mainly on suppression of the critical current of thin superconducting tracks by injection of spin-polarized quasiparticles from a thin-film ferromagnetic layer.[1–4] In most recent work the superconductor has been $YBa_2Cu_3O_x$ (YBCO) and the ferromagnet has been one of the colossal magnetoresistance perovskites $La_{0.67}Ca_{0.33}MnO_3$ (LCMO) or $La_{0.67}Sr_{0.33}MnO_3$ (LSMO). These are chosen because they have a high degree of spin-polarization and because they can be grown epitaxially onto high temperature superconductors (HTS) under very similar growth conditions. This work has been summarized, and the validity (much of it) questioned in a recent paper.[5] Studies have also been made of the critical current of the conventional superconductor niobium[6] and of the penetration depth in YBCO,[7] both as a function of the magnetic state of an overlying ferromagnetic layer. In both cases suppression of the superconducting properties has been observed. There are many theoretical (e.g., Refs. 8 and 9) and experimental studies[10,11] of the current voltage ($I/V$) or conductance-voltage ($G/V$) characteristics of normal metal HTS interfaces, and a few theoretical[12–14] and experimental[15–17] studies on HTS-ferromagnet interfaces. Previous experimental work, although interesting, has also been performed on rather few samples, and these have usually been separately prepared on different substrates. This is unfortunate because there are known to be many problems in forming interfaces between the various perovskite materials. Here we report studies of a range of junctions between YBCO and LCMO or YBCO and LSMO prepared on only five substrates. We have also made comparisons to the behavior of interfaces between YBCO and the nonmagnetic perovskite $LaNiO_3$ (LNO), between YBCO and gold, and between LCMO and LNO. Altogether we have measured 59 junctions prepared on seven substrates.

## II. EXPERIMENTAL METHOD

We describe here the method used for producing the "vertical-geometry" LCMO-YBCO samples, but the same method was used for LSMO, LNO, and Au. All samples were grown using pulsed laser deposition onto 5 mm square $SrTiO_3$ (STO) substrates, with $c$ axis perpendicular to plane. X-ray diffraction showed good epitaxy of all layers. The sample geometry is shown in Fig. 1(a). A layer of YBCO was deposited followed by an *in situ* grown layer of STO. The STO was then patterned and ion beam milled using end-point detection to open 15 vias $\sim 7$ $\mu$m diam around a large central 2 mm square via. A layer of LCMO was then deposited in order to produce electrical contacts to the YBCO underneath. The LCMO was then covered with about 1 $\mu$m thick Au layer in a plasma sputterer. The film was patterned and both Au and LCMO removed by ion milling to leave 0.5 mm square contact pads above the seven square micron junctions and a 2 mm square pad over the central junction [see Fig. 1(a)]. Finally, silver paste was used to connect wires to the gold pads. Silver paste was used in preference to wire bonding, in order to avoid any danger of damaging the LCMO-YBCO interface and also to ensure that the contacts formed equipotential surfaces. Two configurations of junction were used to make electrical measurements. In Fig. 1(b) we show the method used to measure the $I/V$ characteristics. We expect the characteristics to be dominated almost entirely by the smaller junction because of the very high ($\sim 10^5$) ratio of the large to small junction areas. In Fig. 1(c) we show the method used to make a crude estimate of the resistivity of the underlying YBCO and to determine the critical temperature $T_c$ of the film.

One further sample was made in a "cross-geometry" and is shown schematically in Fig. 2. The lower layer is YBCO, and the upper layer is LCMO covered in a sputtered layer of gold to provide a nominally equipotential surface.

 

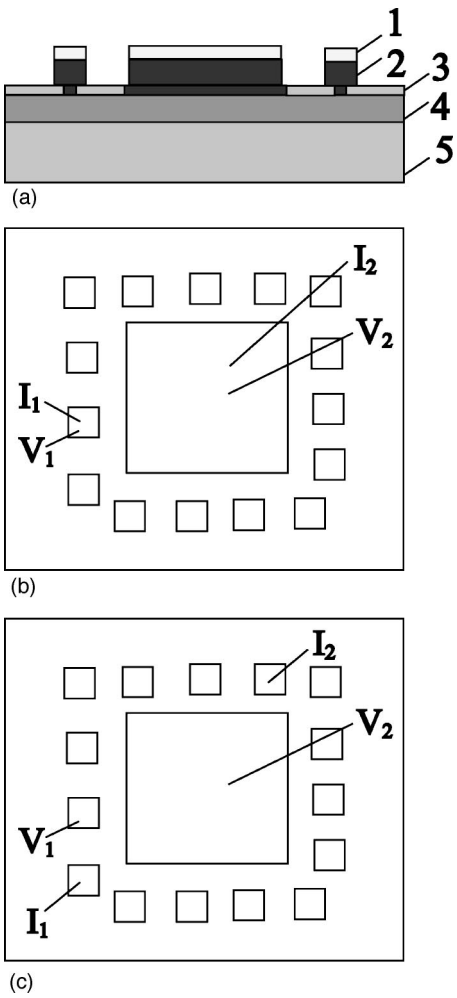


FIG. 1. (a) Side view of specimen. 1: Au, 2: LCMO, 3: STO, 4: YBCO, and 5: STO substrate. (b) Plan view of specimen showing lead connection for measurement of junction resistance. (c) Measurement of resistance of underlying YBCO film. Typical film thicknesses are YBCO 100–200 nm, STO 10–30 nm, and LCMO 100–200 nm.

### III. RESULTS

We consider first the vertical-geometry junctions on which most of our measurements were made. Resistance versus temperature ($R/T$) characteristics for sample 1 are shown in Fig. 3. Measurements on the YBCO resistance $R_{\mathrm{YBCO}}$ show quasilinear behavior with a transition to the superconducting state that starts at around 75 K ($T^{on}$) and is complete

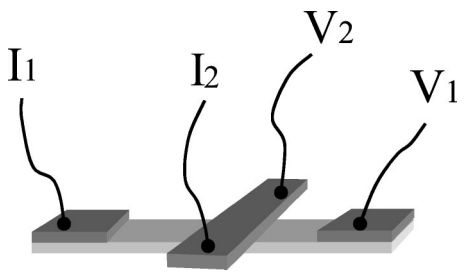


FIG. 2. Cross-geometry of LCMO-YBCO contacts.

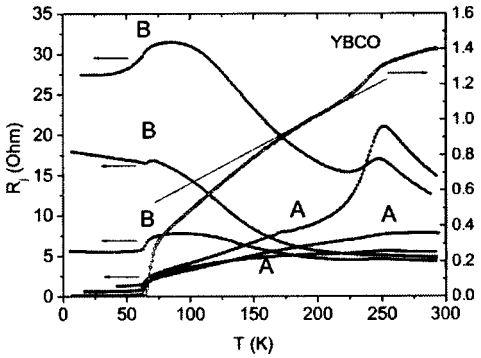


FIG. 3. Resistance vs temperature characteristics $R_j(T)$ of six junctions and of the underlying YBCO film $R_{\mathrm{YBCO}}(T)$ in sample 1.

at around 60 K ($T_c$). This broadened behavior with a low $T_c$ is a common feature of YBCO grown under LCMO. We have found that the $T_c$ of the YBCO can be increased somewhat by annealing in oxygen, so the suppression is likely to be due to underdoping. This means that our samples might be expected to show pseudogap behavior at relatively high temperatures. Although our four-point resistance measurement of $R_{\mathrm{YBCO}}$ is primarily sensitive to the YBCO layer, there is a small but finite transfer length over which current flow changes between the YBCO and LCMO layers. This inevitably convolves in some of the LCMO behavior with that of the YBCO. We are not, therefore, surprised to find that there is also a slight hump in $R_{\mathrm{YBCO}}$ around 260 K that we attribute to the resistance peak in the LCMO. Magnetization measurements on separate LCMO on STO samples confirm that the hump is close to the Curie temperature of the LCMO ~260 K. Such humps are also seen in most measurements of the junction resistance and, in these cases, arise from the series contribution of the LCMO to the total measured resistance.

In Fig. 3 we also show the junction resistance $R_j$ versus temperature for a number of junctions. We identify two types of behavior. In type A junctions, the resistance falls or rises slightly above its room temperature value, before falling as the temperature is reduced toward $T^{on}$. In type B junctions, $R_j$ rises at first slowly as the temperature is reduced, but then rises much more rapidly below some characteristic temperature $T^*$ in the range 150–200 K. At this stage we treat $T^*$ only as a convenient parameter to describe the observed behavior.

We note that in the cross-geometry (Fig. 2) considerable care is needed in the deduction of interface resistance from $I/V$ measurements. It has been pointed out by a number of authors (e.g., Refs. 18–20) how rising, falling, and even negative resistances can arise from changes only in the sheet resistance of the upper and lower layers. Almost all the measurements we discuss here, however were made in the "vertical" geometry. This is a two-point measurement, where such problems do not arise, although we need to be mindful of changes in the YBCO sheet resistance in our interpretation.

The room-temperature resistivity of a good LCMO thin film is $\sim 10^{-3}\ \Omega\ \mathrm{cm}^2$, which would provide a contribution to the junction resistance of 20–40 mΩ (see Figs. 3 and 6). Our

measurements of $R_{\mathrm{YBCO}}$ imply a spreading resistance for our junctions of $1-2\ \Omega$. The sum of these resistances is less than the total contact resistance for our junctions and implies an additional resistance of typically a few ohms at room temperature, associated with the interface itself.

We emphasize that all the data shown in Fig. 3 is taken from junctions on the same sample. The sharp drop in resistance takes place at around 60 K, essentially the same temperature for all samples, and is at the $T_c$ of the YBCO layer. We also have measurements from many samples that confirm the uniformity of our LCMO deposition. We therefore attribute the marked difference between the different $R_j$ curves to the accuracy with which we have milled away the STO interlayer in different parts of the sample. Indeed the change from type A to type B behavior occurs as the junction position moves from one side of the sample to the other; those on the top left, for example, showing dominantly type A behavior, and those toward the bottom right showing type B. STO thickness is a parameter to which we would expect $R_j$ to be particularly sensitive if any sort of tunnelling is involved and our end-point detection is only accurate to around $1-2$ nm. The dramatic change in behavior resulting from such small changes in the extent of the milling strongly argues against any of our observed behavior resulting from direct magnetic effects of the colossal magnetoresistive materials (CMR) on the YBCO. Flux lines created at magnetic domain boundaries would be an obvious possibility. Such behavior was ruled out in Ref. 7 by deliberately introducing a very thin STO layer (much thinner than the expected size of the magnetic domains) between the LCMO and YBCO and showing that the influence of the LCMO layer was removed.

In Fig. 4 we plot the conductance-voltage ($G/V$) curves for two junctions, which show type A behavior. There are three identifiable features: sharp central peak, broad shoulder, and weak parabolic background. The parabolic background is a very common feature of junctions between HTS and normal metals[8] and is also seen in HTS-LCMO junctions reported in other works.[11,16,10] We have also measured LCMO-YBCO junctions on a (110) oriented YBCO film and find a zero bias conductance peak (ZBCP), but no parabolic background. Similar behavior has been reported in a junction between normal metal (Al) and the (110) oriented face of a $La_{2-x}Sr_xCuO_4$ crystal.[10] This suggests that the parabolic background is a property of *c*-axis tunneling.

The narrow central peak disappears above $T^{on}$ and is therefore a feature of the superconducting state. It is comparable in width or lower than twice the gap voltage in optimally doped YBCO ($\sim$24 mV) and is tempting to associate it with the Andreev reflection.[8] However, some samples show an unusually narrow central peak in the sub-mV region, which is clearly not consistent with the gap voltage. A more plausible explanation is that the gap arises from Andreev bound states.[8] These result in narrow, high peaks, and are specific to *d*-wave superconductors in the case of finite transparency of the interface barrier. Such peaks are also specific to tunneling into the *ab* plane[10] and, in our *c*-axis films, *ab* junctions result from the roughness of the interface. Indeed, we find that the peaks become rapidly suppressed in films about 100 nm, where AFM measurements show them to be rather smoother.

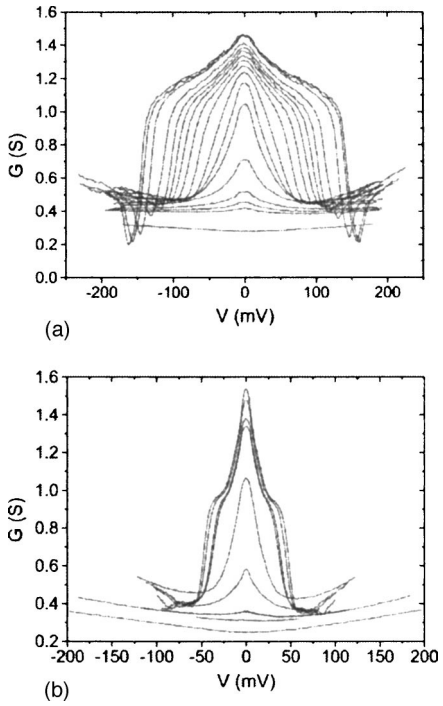


FIG. 4. Conductance vs voltage curves for two LCMO-YBCO junctions of type A at temperatures in order of the decrease of the amplitude: (a) 8.8, 19.1, 32.9, 41.6, 46.3, 48.9, 51.4, 54.3, 57.1, 59.5, 60.8, 61.6, 63.0, 65.2, 66.8, 68.9, and 97.7 K; and (b) 18.7, 32.6, 41.7, 44.6, 59.4, 64.4, 68.6, 73.1, and 96.9 K. The broad shoulder disappears at around the $T_c$ of the YBCO $\sim$62 K.

The broad shoulder is in addition to the narrow central peak and hence represents a parallel conductance path. It merges into the narrow peak at around the $T_c$ of the YBCO and is therefore associated with the fully superconducting state. In some samples the shoulder extends up to 130 meV, but typically it is about 50 meV, still higher than $\Delta$ for optimally doped YBCO.

The sharp drop away from the broad shoulder is similar to that observed in Ref. 16, where it was associated with the nonequilibrium effects of spin-polarized injection. In order to test this interpretation, we prepared sample 2, which had the nonmagnetic homolog LNO in place of the LCMO. All junctions showed type A behavior with $R_j(T)$ falling below room temperature before dropping sharply at the $T_c$ of YBCO [Fig. 5(b)], and $G/V$, showing a narrow central peak and a broad shoulder [Fig. 5(a)].

We also prepared sample 3, which had direct YBCO-gold junctions only. Despite the much higher junction resistance ($\sim 4\times 10^{-5}\ \Omega\ \mathrm{cm}^2$) typical of gold-HTS interfaces,[23] sample 3 again showed type-A behavior in the $R_j(T)$ [Fig. 6(b)] and $G/V$ [Fig. 6(a)] characteristics.

In summary, we find that almost all our samples that show type A behavior, also show $G/V$ characteristics with a narrow central peak and a broad shoulder, which falls abruptly down into a parabolic behavior at higher voltages, irrespective of whether samples have a ferromagnetic layer or not. The $G/V$ behavior of type-A samples cannot, therefore, have anything to do with the spin-polarized nature of the injected electrons.

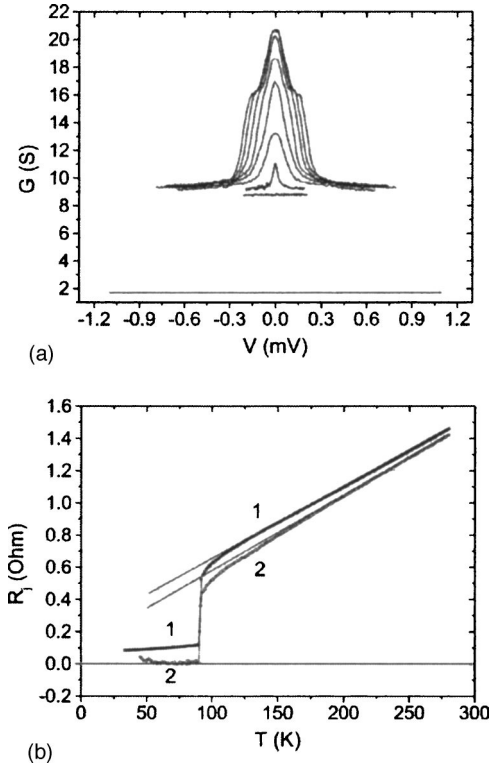


FIG. 5. (a) Conductance-voltage curves for a LNO-YBCO sample at temperatures (up to down) 18.8, 32.8, 41.8, 50.7, 59.6, 68.9, 78.2, and 86.9 K, and (b) junction resistance vs temperature for measuring current 8 mA (1) and 70 $\mu$A (2). Note the much lower $R_j$ than in the LCMO-YBCO sample 1.

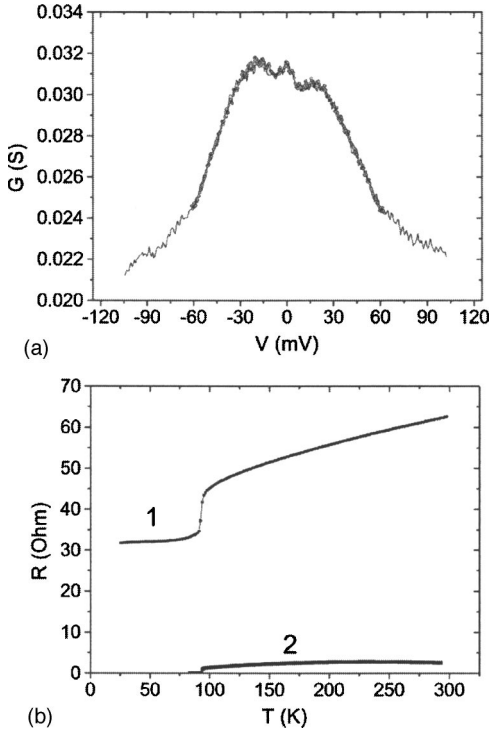


FIG. 6. (a) Two consecutive conductance/voltage curves at 18.8 K and (b) junction 1 and YBCO 2 resistance vs temperature for a gold-YBCO sample. Note the much higher $R$ of the junction than in the LCMO/YBCO sample 1.

An alternative explanation for the broad shoulder is heating by the measuring current. In Fig. 4 the abrupt fall on the shoulder occurs at around 130 mV. The power dissipated in the junction is only $\sim$17 mW, but it may be dissipated over an area of only $5\times10^{-11}$ m$^2$, giving a power density $\sim3\times10^8$ W m$^{-2}$. It is known that $\sim10^7$ W m$^{-2}$ is sufficient to cause a temperature rise $\sim$1 K between a film of YBCO and the underlying STO substrate,[24] so heating at such power densities could be a serious complication. Heating fails, however, to explain why the sharp fall shown in Fig. 4(b) occurs at much lower power density than in Fig. 4(a) and, indeed, why it is seen at all in the YBCO-gold junctions [Fig. 6(b)], where the conductance below $T_c$ and hence the power dissipated at a given voltage, is some two orders-of-magnitude lower than in the LCMO-YBCO junctions. Heating also fails to explain why the conductance above the sharp drop falls rather than rises with increasing voltage, as would be expected from the positive slope in $R_{\mathrm{YBCO}}(T)$.

Another possible explanation of the shoulder is that the current density in the YBCO at the junction becomes sufficiently high that it exceeds the critical current. The current density at the shoulder in Fig. 4(a) is $\sim3\times10^9$ A m$^{-2}$, a plausible figure for the $J_c$ of underdoped YBCO. As the current exceeds $J_c$, a region of quasinormal YBCO spreads radially outward from the junction. We have devoted some effort to computer modeling this behavior, but no satisfactory fit to the data has been found. We also note that the broad shoulder is seen in a wide range of contacts where the current at the shoulder differs by a factor of up to 150. Our model also fails to explain why the conductance continues to rise above the sharp drop, nor why the central peak is apparently unaffected by the presence of the shoulder. We therefore conclude that suppression of superconductivity by the critical current is an unlikely explanation.

We have many junctions showing similar behavior, but the range of power and current densities at which various features occur does not point to a common explanation based on either heating or critical current effects.

An interesting feature of the broad shoulder is that in almost all samples it exhibits approximately the factor of 2 drop in conductance characteristic of Andreev reflection, albeit at higher voltage than expected. It is well known that $\Delta$ increases with underdoping.[21] The value of 50 meV is a typical value for $T_c$ about 60 K,[21] so severe underdoping at the interface could be responsible for the voltages at which the shoulders are observed. The presence of a ZBCP in any contacts between YBCO and LCMO is, however, surprising, since Andreev reflection is not expected for a highly spin-polarized ferromagnet such as LCMO; the reflected hole is of opposite spin to the incident electron and therefore has a negligible density of states available to it in the required spin band. If the above interpretation is correct, it would imply that the LCMO samples suffer strong depolarization of the spins at the interface in contacts of type A.

We consider now the junctions of sample 1 that display a rising $R_j$ below $T^*$ (type B). We find that these junctions show only a broad parabolic background in their $G/V$ behavior, with no evidence of a ZBCP or shoulder. It is tempting to

assume that both the rising resistance below $T^*$ and the absence of a ZBCP and a shoulder are simply a consequence of a high series resistance $R_s$ due to a very thin unmilled layer of STO. It is easy to show that the effect of such a series resistance on these features would be to reduce their amplitude and broaden the voltage scale by the same factor of approximately $R_s/R_j(0)$, where $R_j(0)$ is $1/G(V=0)$. We see no evidence of such an effect in the many junctions measured, so this is unlikely to be the explanation. In sample 4 (LCMO/YBCO) we deliberately milled a few nanometers into the YBCO in order to ensure that there was no intermediate STO layer. Contrary to our expectation, junctions on this sample were all of type B with $R_j$ rising below a temperature $T^*$, again in the range 150–200 K. We found a very small ZBCP in only one of the eight measured junctions. The implication of this result is that type-B behavior does not arise from an unmilled layer of STO, but that it is observed in those junctions that are more deeply milled and have better physical contact between the layers.

We have argued above that spin-polarization is not responsible for type-A behavior. We now consider the possibility that the rising resistance below $T^*$ and the absence of either a sharp peak or a broad shoulder in type-B samples is related to the spin-polarization of the current flow from the LCMO layer. It has been pointed out by Gim *et al.*[5] that it is a nontrivial matter to distinguish the effects of spin-polarization from nonpolarized quasiparticle injection or from spurious effects, such as heating or simple current addition in a nonlinear system. An interesting approach reported in other works has been to take the ferromagnet around its magnetic hysteresis loop with a magnetic field $H$ applied parallel to the plane of the film. In one work the critical current of the niobium in a niobium-cobalt bilayer was studied as a function of magnetic field,[25] and in the other the penetration depth of YBCO was measured in a LCMO-YBCO bilayer.[7] In both cases superconductivity was enhanced at the coercive field of the ferromagnet. It was argued that this was because of the partial cancellation of any effects due to spin-polarization close to the magnetic domain walls. This cancellation would be enhanced at the coercive field where the magnetic domain size is small and the area of domain wall is maximal. We have therefore followed the same procedure, using a magnetic field parallel to the plane of the film. A steady current of 3 mA was passed through the junction, and voltage was measured as a function of $H$ at a series of temperatures. The results for one LSMO-YBCO sample of type B are shown in Fig. 7. At all temperatures below $T^*$, down to our lowest measurement temperature, we find that there are small, but significant peaks in the voltage at the coercive field of the LSMO.

The fractional size of the peaks rises slowly as the temperature is decreased, but shows no obvious change as the temperature is reduced below the superconducting transition of the YBCO layer (Fig. 8).

With few exceptions we find that type-B junctions (which show a rising $R_j$ below some characteristic temperature $T^*$) also show double hysteresis peaks in the $R_j(H)$ characteristics, but no ZBCP or broad shoulder. Junctions of type A (which have $R_j$ that is dominantly falling below room temperature) show no peaks in $R_j(H)$, but do show ZBCPs and broad shoulders in the $G/V$ characteristics. These effects are, therefore, mutually exclusive.

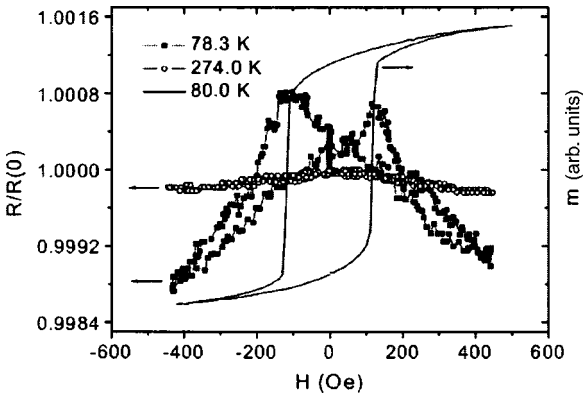


FIG. 7. Normalized voltage (or normalized resistance) vs field at 3 mA for a junction of type B in the YBCO-LSMO sample 5, at two temperatures: 78.3 K, which is below $T^*$, and 274.0 K, which is above $T^*$. The magnetization curve at 80.0 K for the same sample is also shown.

We now consider possible interpretations of our results. The $R_j/H$ behavior of type-B junctions below $T^*$ is highly reminiscent of that shown by LCMO grown on bicrystal substrates and by LCMO films having a mosaic spread of around 1°.[26] The peaks occur close to the coercive field of the LCMO and are believed to be associated with a field-dependent alignment of adjacent single-domain crystallites. The effects disappear above $T_{\mathrm{Curie}}$ as expected.

In type-B junctions (which were more deeply milled) there is no STO left, and we expect good physical contact between the LC(S)MO and YBCO layers. It is known that an LSMO free surface has a suppressed magnetization in the first few nanometers,[27] reaching the bulk value at temperature about 100 K. The magnetization of LSMO-insulator interfaces is more robust, but even in this case is suppressed down to 60 K below the bulk value.[28] An additional factor in LCMO-YBCO interfaces is diffusion of Y,[29] which may lead to a further decrease of $T_{\mathrm{Curie}}$. The resistivity of LCMO shows a strong rise with decreasing $T_{\mathrm{Curie}}$ (Ref. 30), and a suitable range of seriously suppressed $T_{\mathrm{Curie}}$ values could be

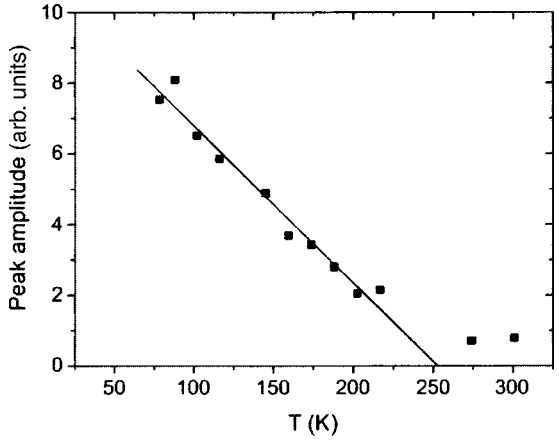


FIG. 8. Amplitude of peaks in $R_j(H)$ vs temperature for an LSMO-YBCO junction of type B.

responsible for the rapidly rising $R_j$ observed below $T^*$ in type-B samples.

The peaks in the $R_j/H$ characteristics can also be explained by the physical properties of the interface. The ion-beam milling of YBCO may produce surface damage that could result in irregular growth in subsequent layers close to the interface. We would expect any such effect to be more pronounced in the deeply milled sample type-B contacts. Only a small amount of physical disorder of the form seen in bicrystal and 1° mosaic spread LCMO films[26] may be needed to produce the very small peaks we observe. This model could provide an explanation for the correlation between the high $R_j$ values at low temperatures and the $R_j(H)$ peaks below the same temperature $T^*$, which we identify with the lower range of the suppressed $T_{\text{Curie}}$. Both effects would be expected to disappear above $T^*$, as observed.

In type-A junctions, the milling was less deep, and a very thin surface layer of STO may remain. We would therefore expect much less chemical interaction between the YBCO layers than in type-B junctions and, hence, a negligible layer with suppressed $T_{\text{Curie}}$. We would also expect less damage to the crystallinity of the YBCO and, hence, of the LCMO at the interface than in type-B samples. Peaks in $R_j(H)$ would therefore not occur. An exception to this behavior is sample 6, where we have retained LCMO as the upper layer, but have replaced the lower YBCO layer with LNO. The 7 $\mu$m holes were again deeply milled, but here we find type-A behavior, i.e., falling junction resistance at low temperatures. This sample, however, showed peaks in $R_j(H)$, albeit at considerably higher magnetic field ($\sim$400 Oe) than the other samples. This behavior may well be explained by the above model.

There are, however, a number of unsatisfactory features of this model. First, it requires that the supposed layer of STO in type-A samples is sufficiently thick to prevent chemical diffusion or microstructural damage, but that it is, at the same time, sufficiently thin to offer negligible series resistance at low temperatures. Some special pleading is also required for a distribution of Curie temperatures that will provide the monotonically rising $R_j$ in type-B junctions, but still show a hump at around the $T_{\text{Curie}}$ of bulk samples (see Fig. 3). We also require that the resistance at low temperatures is dominated by the damaged LCMO layer, but at the same time the peaks in $R_j(H)$ are very small, only $\sim$2% the size found in bicrystal and 1° LCMO films. All our junctions show a distinct change in the slope of $R_j(T)$ below $T_c$, which is again unexpected if the behavior is dominated by the properties of the LCMO. We also need to explain why the peaks in $R_j(H)$ occur at the coercive field of bulk LCMO, if they result from an interface where the magnetic properties are supposedly suppressed. A further objection to our model comes from $R_j(T)$ of the YBCO-LSMO sample 5, where we replaced LCMO with LSMO (see Fig. 9). This sample is also deep milled and shows junctions of type B. The Curie temperature for our LSMO samples is $\sim$350 K, some 90 K higher than for LCMO. We see from Fig. 9, however, that the temperature $T^*$, below which $R_j$ starts to rise substantially, is very similar to that for the LCMO-YBCO samples shown in Fig. 3. This sample also shows peaks in the $R_j/H$ characteristics, which again disappear above a $T^* \sim 150-200$ K. The very similar values of $T^*$ shown by the LCMO and LSMO samples implies that neither the rising $R_j$ nor the peaks in $R_j(H)$ are simply properties of the CMR layer. We deduce that the observed behavior arises from the electronic properties of the CMR-YBCO interface or from the YBCO immediately under the interface, and not from the CMR alone, as suggested above, nor from any direct magnetic interaction for the reasons given earlier.

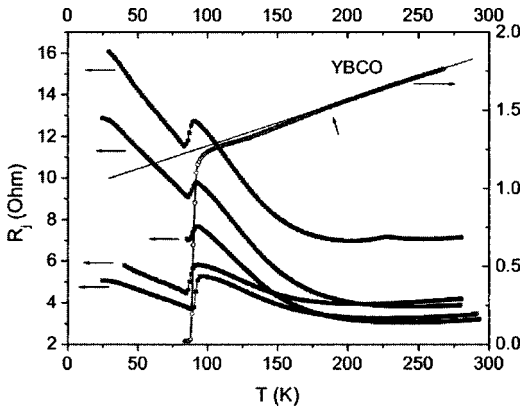


FIG. 9. $R_j(T)$ and $R_{\text{YBCO}}(T)$ for the LSMO-YBCO sample 5.

We consider an alternative possible explanation for our results. We assume that the LC(S)MO layers display substantial spin-polarization up to their bulk Curie temperatures. We have noted that all our samples have low $T_c$'s and would therefore be expected to have high pseudogap temperatures; indeed, a sample with $T_c$ of 60 K would be expected to have a pseudogap temperature around 200 K.[21,31]

Almost all of our $R_{\text{YBCO}}(T)$ curves show a deviation of $R_{\text{YBCO}}(T)$ from linear behavior at 150–200 K, as shown by adding a straight line to $R_{\text{YBCO}}(T)$ in Figs. 9 and 3. Such behavior has been sited in many works as evidence of pseudogap behavior.[31–34] We tentatively suggest that our temperature $T^*$ can be identified with the pseudogap temperature and further that our results in type-B junctions, where the interlayer contact is good, show the effect of injection from the spin-polarized state of the CMR layer into the pseudogap state of the YBCO. The effect of spin-polarized injection on the pseudogap state has not been explored, either experimentally or theoretically, so we will see what can be deduced from our data if we make the assumption that this is, indeed, the case.

Type B junctions do not occur in Au-YBCO or LNO-YBCO junctions and therefore reflect the interaction of the ferromagnetic layer with the pseudogap state. It was argued[7,25] that the enhancement of superconductivity at the coercive field of the ferromagnetic layer was due to a partial cancellation of the spin polarization at the magnetic domain boundaries. The expected size of magnetic domains in our films is $<1$ $\mu$m,[40] so some domain walls should be present our 7 $\mu$m square junctions. It immediately follows that the rising resistance below $T^*$ and the peaks in $R_j(H)$ cannot have a single cause—if spin-polarization results in an enhanced resistance in $R_j(T)$ below $T^*$, then it cannot also cause peaks in $R_j(H)$.

We consider first the $R_j(T)$ behavior. Systematic measurements of the resistivity of YBCO at various doping levels imply that the effect of the pseudogap state is to reduce the resistivity below that which would be expected in the absence of pseudogap effects,[31,33] and this effect is quite small—at most 10% at $T_c$. Suppression of the pseudogap state by the injection of polarized spins could, therefore, only result in a suppression in the rate of fall in $R_j(T)$ with decreasing temperature and not the strong rise that we observe in type-B samples. Possible explanations for the rising resistance are an enhancement of the scattering rate for spin-polarized electrons in the YBCO by the antiferromagnetic fluctuations associated with the pseudogap state[35–39] or a reduction in the tunneling rate through some residual barrier between the ferromagnetic and superconducting layers. A quite different theory for the pseudogap state is that it results from the formation of preformed but incoherent pairs, coherence only existing below the $T_c$ of the YBCO.[41] It has also been argued that Andreev reflection from the pseudogap state would be expected, if this is indeed the case.[22] This could again lead to an enhanced resistance below the pseudogap temperature because of the suppression of Andreev reflection by the spin-polarized state of the ferromagnetic layer. The rather pronounced peaks in $R_j(H)$ at the coercive field are harder to explain. They could occur if corresponding domains were induced in the pseudogap state of the YBCO and a domain-domain interface resistance was present, analogous to that which occurs in CMR films and bulk materials,[26,30] only of much smaller magnitude. We have no detailed model, and, in the absence of any proper theory, these suggestions must remain speculative. We note that gaplike structures in the $G/V$ characteristics have been reported above $T_c$ in tunnel junctions prepared by *in situ* cleaving[42] or break junctions.[43] Our samples are designed to study the injection of polarized spins across a direct contact. We, therefore, have no reason to expect similar characteristics, and our arguments for pseudogap behavior are quite different.

We turn, finally to the single cross-geometry sample, which shows characteristic type-B behavior, with rising $R_{\mathrm{YBCO}}(T)$ below a characteristic temperature $T^*$ and the usual peaks in $R_j(H)$. We recall our earlier comments on the difficulties of deducing interface resistances in this geometry, in particular, that a rising $R_{\mathrm{YBCO}}(T)$ is not necessarily a characteristic of the interface alone. However, this is not the important issue here, which is the dependence of $R_j(H)$ on the state of oxygenation of the sample. In Fig. 10 we show the peak height as a function of temperature for three states of the sample. Curve 1 is for the as prepared sample; curve 2, the sample after seven months in a dry box at room temperature; and curve 3, the same sample after finally annealing in flowing oxygen for 12 h at 550 °C. We have no way of measuring the oxygenation state of the interface, but it seems highly plausible that curve 3 represents the most highly oxygenated state and curve 2, the least. In view of the very limited data on this sample (which eventually suffered a misfortune), we would be reluctant to read too much into the results. We note, however, that the order of the three data sets is entirely consistent with a picture based on pseudogap behavior: higher oxygenation of the interface results in a reduced value of $T^*$.

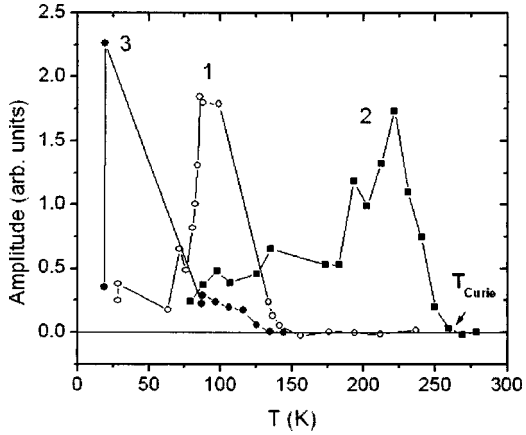


FIG. 10. Temperature dependence of the amplitude of the coercive-field anomaly in the crosslike LCMO-YBCO contact.

This is exactly the opposite of what we would expect if the effect were due to a degraded LCMO layer, where improved oxygenation increases $T_{\mathrm{Curie}}$.

The real test of our hypothesis would clearly be to systematically relate $R_j(T)$ and $R_{\mathrm{YBCO}}(T)$ and $R_{\mathrm{LCMO}}(T)$ to the oxygenation state of our films. Unfortunately, our present samples and their mounting do not lend themselves to this. Work is in progress to make such a study in a geometry that will also enable us to distinguish between interface and YBCO film effects.

## IV. CONCLUSIONS

We report measurements of the resistance of a large number of 7 $\mu$m junctions on a range of bilayers between YBCO and CMR, and LNO and gold layers. We find that the samples that show a dominantly falling resistance as the temperature is reduced from 300 K display zero bias conductance peaks and a broad shoulder, both of which disappear above $T_c$. We find that heating and critical current effects do not provide a satisfactory explanation for our observations; they associate the sharp peak with Andreev bound states and the broad shoulder with Andreev reflection at an enhanced voltage, which is enhanced by a deoxygenated interface layer. Those samples that show a rising resistance below a characteristic temperature $T^*$ do not display zero bias anomalies, but do show peaks in $R_j(H)$ below $T^*$. We have considered models based on the properties of the CMR alone and find that these do not provide a satisfactory explanation of our results. We have tentatively associated $T^*$ with the pseudogap temperature and have suggested a number of tentative models to explain the observed behavior. Preliminary measurements of a single sample in a cross-type geometry are again consistent with an explanation based on pseudogap behavior. We have identified the need for a systematic study of interface properties over a range of doping levels.

## ACKNOWLEDGMENTS

We thank Dr. R. Chakalov for preparation of thin films.

[1] V. A. Vas'ko, V. A. Larkin, P. A. Kraus, K. R. Nikolaev, D. E. Grupp, C. A. Nordman, and A. M. Goldman, Phys. Rev. Lett. **78**, 1134 (1997).
[2] Z. W. Dong, R. Ramesh, T. Venkatesan, M. Johnson, Z. Y. Chen, S. P. Pai, V. Talyansky, R. P. Sharma, R. Shreekala, C. J. Lobb, and R. L. Greene, Appl. Phys. Lett. **71**, 1718 (1997).
[3] N. C. Yeh, R. P. Vasquez, C. C. Fu, A. V. Samoilov, Y. Li, and K. Vakili, Phys. Rev. B **60**, 10 522 (1999).
[4] R. M. Stroud, J. Kim, C. R. Eddy, D. B. Chrisey, J. S. Horwitz, D. Koller, M. S. Osofsky, R. J. Soulen, Jr., and R. C. Y. Auyeung, J. Appl. Phys. **83**, 7189 (1998).
[5] Y. Gim, A. W. Kliensasser, and J. B. Barner, J. Appl. Phys. **90**, 4063 (2001).
[6] M. D. P. M. Tedrow and R. Meservey, Phys. Rev. Lett. **26**, 192 (1971); **37**, 858 (1976).
[7] M. D. Allsworth, R. A. Chakalov, P. Mikheenko, M. S. Colclough, and C. M. Muirhead, Appl. Phys. Lett. **80**, 4196 (2002).
[8] S. Kashiwaya and Y. Tanaka, Rep. Prog. Phys. **63**, 1641 (2000).
[9] Y. Asano and Y. Tanaka, Phys. Rev. B **65**, 064522 (2002).
[10] Y. Dagan, A. Kohen, G. Deutscher, and A. Revcolevschi, Phys. Rev. B **61**, 7012 (2000).
[11] Wan Wang, M. Yamazaki, K. Lee, and I. Iguchi, Phys. Rev. B **60**, 4272 (1999).
[12] J.-X. Zhu and C. S. Ting, Phys. Rev. B **61**, 1456 (2000).
[13] Z. C. Dong, D. Y. Xing, Z. D. Wang, Z. Zheng, and J. Dong, Phys. Rev. B **63**, 144520 (2001).
[14] T. Hirai, Y. Tanaka, N. Yoshida, Y. Asano, J. Inoue, and S. Kashiwaya, Phys. Rev. B **67**, 174501 (2003).
[15] A. Sawa, S. Kashiwaya, H. Obara, H. Yamasaki, M. Koyanagi, and Y. Tanaka, Physica B **284–288**, 493 (2000).
[16] P. A. Kraus, A. Bhattacharya, and A. M. Goldman, Phys. Rev. B **64**, 220505(R) (2001).
[17] Z. Y. Chen, A. Biswas, I. Zutic, T. Wu, S. B. Ogale, R. L. Greene, and T. Venkatesan, Phys. Rev. B **63**, 212508 (2001).
[18] R. J. Pedersen and F. L. Vernon, Jr., Appl. Phys. Lett. **10**, 29 (1967).
[19] I. Iguchi, T. Kusumori, and H. Hayashida, Jpn. J. Appl. Phys., Part 1 **32**, 3442 (1993).
[20] R. J. M. van de Veerdonk, J. Nowak, R. Meservey, J. S. Moodera, and W. J. M. de Jonge, Appl. Phys. Lett. **71**, 2839 (1997).
[21] M. Oda, N. Momono, and M. Ido, Supercond. Sci. Technol. **13**, R139 (2000).
[22] H.-Y. Choi, Y. Bang, and D. K. Campbell, Phys. Rev. B **61**, 9748 (2000).
[23] L. Mieville, D. Worledge, T. H. Geballe, R. Contreras, and K. Char, Appl. Phys. Lett. **73**, 1736 (1998).
[24] R. S. Prasher and P. E. Phelan, J. Supercond. **10**, 473 (1997).
[25] R. J. Kinsey, G. Burnell, and M. G. Blamire, IEEE Trans. Appl. Supercond. **11**, 904 (2001).
[26] J. E. Evetts, M. G. Blamire, N. D. Mathur, S. P. Isaac, B.-S. Teo, L. F. Cohen, and J. L. Macmanus-Driscoll, Philos. Trans. R. Soc. London, Ser. A **356**, 1593 (1998).
[27] J.-H. Park, E. Vescovo, H.-J. Kim, C. Kwon, R. Ramesh, and T. Venkatesan, Phys. Rev. Lett. **81**, 1953 (1998).
[28] V. Garcia, M. Bibes, A. Barthelemy, M. Bowen, E. Jacquet, J.-P. Contour, and A. Fert, Phys. Rev. B **69**, 052403 (2004).
[29] W. S. Tan, L. Yang, H. Sha, X. S. Wu, J. Gao, and S. S. Jiang, Surf. Rev. Lett. **10**, 317 (2003).
[30] *Colossal Magnetoresistance, Charge Ordering and Related Properties of Manganese Oxides*, edited by C. N. R. Rao and B. Raveau (World Scientific, Singapore, 1998).
[31] T. Timusk and B. Statt, Rep. Prog. Phys. **62**, 61 (1999).
[32] B. Bucher, P. Steiner, J. Karpinski, E. Kaldis, and P. Wachter, Phys. Rev. Lett. **70**, 2012 (1993).
[33] J. L. Tallon, J. W. Loram, G. V. M. Williams, J. R. Cooper, I. R. Fisher, J. D. Johnson, M. P. Staines, and C. Bernhard, Phys. Status Solidi A **215**, 531 (1999).
[34] V. V. Moshchalkov, J. Vanacken, and L. Trappeniers, Phys. Rev. B **64**, 214504 (2001).
[35] T. Dahm, Phys. Rev. B **61**, 6381 (2000).
[36] P. Dai, H. A. Mook, R. D. Hunt, and F. Dogan, Phys. Rev. B **63**, 054525 (2001).
[37] C. Timm, D. Manske, and K. H. Bennemann, Phys. Rev. B **66**, 094515 (2002).
[38] P. Prelovsek and A. Ramsak, Phys. Rev. B **65**, 174529 (2002).
[39] P. A. Marchetti, L. De Leo, G. Orso, Z. B. Su, and L. Yu, Phys. Rev. B **69**, 024527 (2004).
[40] Y. Wu, Y. Matsushita, and Y. Suzuki, Phys. Rev. B **64**, 220404(R) (2001).
[41] V. J. Emery and S. A. Kivelson, Nature (London) **374**, 434 (1995).
[42] Ch. Renner, B. Revaz, J-Y. Genoud, K. Kadowaki, and O. Fischer, Phys. Rev. Lett. **80**, 149 (1998).
[43] D. Mandrus, L. Forro, D. Koller, and L. Mihaly, Nature (London) **351**, 460 (1991).